ELSEVIER

Coastal Engineering 29 (1996) 79-99

COASTAL ENGINEERING

The growth of fetch limited waves in water of finite depth. Part 2. Spectral evolution

I.R. Young [a], L.A. Verhagen [b]

[a] *School of Civil Engineering, University College, University of N.S.W., Canberra, A.C.T. 2600, Australia*
[b] *HASKONING, P.O. Box 151, 6500 AD Nijmegen, Netherlands*

Received 17 August 1995; accepted 9 February 1996

Abstract

Results showing the evolution of the wave spectrum in finite depth, fetch limited conditions are presented. The data were obtained from a series of eight wave gauges established in shallow Lake George, Australia. The data are well modelled by the previously proposed TMA spectral form and clearly show the transition of the spectra from deep water to depth limited conditions. The TMA parameter of α is found to be a function of the non-dimensional wavenumber, κ but the spectral peak shape parameters of γ and σ appear uncorrelated with κ. The parameter γ is shown to be a function of both non-dimensional fetch, χ and non-dimensional depth, δ. In severely depth limited conditions γ becomes solely a function of δ, increasing in magnitude as δ decreases. Hence, depth limited spectra could be expected to be very peaked compared to deep water counterparts.

1. Introduction

Young and Verhagen (1996) (henceforth referred to as Part 1) described a field experiment aimed at determining an understanding of the fetch limited evolution of surface gravity waves in water of finite depth. In Part 1, a detailed description of the experiment and data processing was presented, along with an investigation of the fetch limited development of the total spectral energy and peak frequency. It is the aim of this paper to present results detailing the evolution of the one-dimensional, finite depth spectrum with fetch.

Investigations of the evolution of deep water fetch limited spectra are now relatively common. In contrast, the case in waters of finite depth is markedly different. Although there have been reported studies of the spectra of wind generated waves (as opposed to swell), to the authors' knowledge, there have been no studies of spectral evolution under well defined fetch limited conditions in water of finite depth.

0378-3839/96/$15.00 Published by Elsevier Science B.V.
PII S0378-3839(96)00007-5

The data from the present Lake George experiment (see Part 1) provide the first opportunity to investigate the detailed form of the finite depth spectrum and its evolution with fetch.

The arrangement of the paper is as follows. Section 2 presents a review of previous investigations of fetch limited spectra in deep water with the limited extensions to finite depth conditions. Section 3 briefly describes the present experiment and data processing. In order to investigate an appropriate functional form for the recorded spectra, a preliminary analysis of the decay of the high frequency portion of the spectrum as a function of frequency is presented in Section 4, followed by the fitting of a full spectral form to the data in Section 5. The evolution of the spectral parameters obtained in Section 5 is investigated in Section 6. The consistency of the derived spectral form with the integral results of Part 1 is investigated in Section 7. As with previous studies of this type, there is significant scatter in the derived spectral parameters and a detailed error analysis is presented in Section 8, to determine the sources of this scatter. Finally conclusions are presented in Section 9.

2. Fetch limited spectral evolution

2.1. Deep water

Based on the pioneering dimensional analysis investigation of the high frequency spectral form by Phillips (1958), Hasselmann et al. (1973) proposed the JONSWAP spectral form to approximate fetch limited spectra recorded in the North Sea,

$$F(f)=\alpha g^{2}(2\pi)^{-4}f^{-5}\exp\left[\frac{-5}{4}\left(\frac{f}{f_{\mathrm{p}}}\right)^{-4}\right]\cdot\gamma^{\exp\left[\frac{-(f-f_{\mathrm{p}})^{2}}{2\sigma^{2}f_{\mathrm{p}}^{2}}\right]} \tag{1}$$

where $F(f)$ is the one-dimensional spectrum and f is frequency. The JONSWAP form (1) is defined in terms of the four spectral parameters, f_{p}, α, γ and σ. The JONSWAP form was an extension of that originally proposed by Pierson and Moskowitz (1964) for fully developed wind sea spectra. The last term in Eq. (1), modifies the Pierson–Moskowitz form for fetch limited conditions. Hasselmann et al. (1973) found that the peak frequency, f_{p} and the "Phillips' parameter", α varied as a function of the non-dimensional fetch, $\chi=gx/u^{2}$, where x is the fetch, u is a measure of the wind speed and g is the gravitational acceleration. The shape parameters, γ and σ, however, exhibited no trend as a function of χ. As a result Hasselmann et al. (1973) adopted their mean values $\gamma=3.3$ and $\sigma=\sigma_{\mathrm{a}}=0.07$ for $f\leq f_{\mathrm{p}}$ and $\sigma=\sigma_{\mathrm{b}}=0.09$ for $f>f_{\mathrm{p}}$.

The validity of the Phillips (1958) high frequency form $F(f)\propto f^{-5}$, upon which the JONSWAP form is based, has been questioned by numerous authors (e.g. Toba, 1973; Kitaigorodskii et al., 1975; Mitsuyasu et al., 1975; Forristall, 1981; Kahma, 1981; Kitaigorodskii, 1983; Battjes et al., 1987; Resio, 1987; Donelan et al., 1985). These studies yielded a variety of powers that described the high frequency tail of the spectrum with exponents varying from -3.5 to -5.0. In a detailed field study of deep water fetch limited spectra, Donelan et al. (1985) presented data supporting an exponent of -4.0. Based on these data, they proposed the spectral form (modified version of JONSWAP)

$$F(f)=\alpha g^{2}(2\pi)^{-4}f^{-4}f_{p}^{-1}\exp\left[-\left(\frac{f}{f_{p}}\right)^{-4}\right]\cdot\gamma^{\exp\left[\frac{-(f-f_{p})^{2}}{2\sigma^{2}f_{p}^{2}}\right]} \tag{2}$$

Due to the difficulty of determining the fetch, x accurately, Donelan et al. (1985) parameterized the spectral parameters of Eq. (2) in terms of the inverse wave age, U_{10}/C_{p}, where U_{10} is the wind speed measured at a reference height of 10 m and C_{p} is the phase speed of components at the spectral peak frequency. They found that α, γ and the non-dimensional energy, $\epsilon=g^{2}E/U_{10}^{4}$ scaled in terms of U_{10}/C_{p}. The final parameter σ was determined such that the total spectral energy, $E=\int F(f)\mathrm{d}f$ obtained from the spectral form (Eq. (2)) was equal to the observed relationship between ϵ and U_{10}/C_{p}.

Although the results of Donelan et al. (1985) suggest a high frequency form proportional to f^{-4} rather than f^{-5}, the debate still continues as to the most appropriate form. Hasselmann et al. (1973) first speculated that it was the process of nonlinear interactions which was responsible for the existence of the ordered high frequency tail. This was confirmed by Young and Van Vledder (1993) who clearly demonstrated the shape stabilizing influence of nonlinear interactions within the spectrum. In a more detailed study Banner and Young (1994) confirmed that the nonlinear terms were dominant but also showed that the other processes of atmospheric input and "white-cap" dissipation were also significant in determining the detailed form of the high frequency spectral tail. Banner (1990) has presented stereo-photographic data which suggests that the universal high frequency form exists in the wind direction slice of the wavenumber spectrum. Hence, the form of the frequency spectrum will depend on the directional spreading as well as the peak enhancement (value of γ), as this controls the degree of Doppler shifting of the high frequency components in the spectral tail.

These considerations cast some doubt on the existence of a universal shape of the form f^{n} for the high frequency region of the frequency spectrum, even in deep water. Nevertheless, the very significant composite data set suggests the exponent is between -4 and -5.

2.2. Finite depth water

In contrast to the wealth of observed deep water fetch limited spectra, the data set in finite depth situations is very small. The well known fetch limited finite depth field experiments of Lake Okeechobe (U.S. Army Corps of Engineers, 1955; Bretschneider, 1958) and Lake Marken (Bouws, 1986) reported only on the development of the integral spectral properties of total energy and peak spectral frequency (see Part 1).

The most comprehensive study of finite depth wave spectra is that of Bouws et al. (1985, 1987). This study considered the, so called, TMA data set, comprised of measurements made at coastal sites during three separate field experiments (TEXEL — Dutch North Sea; MARSEN — German Bight; ARSLOE — US east coast). In all cases, the spectra could be described as wind sea spectra, in that no significant swell was present. As no clear fetch could be delineated in many of the cases, it is difficult to determine whether they were fetch limited. Following Kitaigorodskii (1962) and Kitaigorodskii et al. (1975), they assumed that a universal spectral form existed in the wavenumber spectrum given by

$$F(k)=\frac{\alpha}{2}k^{-3}\Psi(k,f_p,d) \tag{3}$$

where $F(k)$ is the wavenumber spectrum, k is the wavenumber and Ψ is a non-dimensional shape function which approaches one for $k \gg k_p$ where k_p is the wavenumber of the spectral peak. When converted to a frequency spectrum using linear wave theory, Eq. (3) produces a form with a variable high frequency exponent. In deep water it will be -5 and at the shallow water limit -3.

Assuming a shape function of the JONSWAP form (Hasselmann et al., 1973), Eq. (3) produces a frequency spectrum of the form

$$E(f)=\alpha g^2(2\pi)^{-4}f^{-5}\exp\left[\frac{-5}{4}\left(\frac{f}{f_p}\right)^{-4}\right]\cdot\gamma^{\exp\left[\frac{-(f-f_p)^2}{2\sigma^2 f_p^2}\right]}\cdot\Phi \tag{4}$$

and

$$\Phi=\left\{\frac{[k(f,d)]^{-3}\cdot\dfrac{\partial k(f,d)}{\partial f}}{[k(f,\infty)]^{-3}\cdot\dfrac{\partial k(f,\infty)}{\partial f}}\right\} \tag{5}$$

Eq. (4) was termed the TMA spectral form by Bouws et al. (1985). Disregarding the shape function in Eq. (3), Bouws et al. (1985) determined an approximation to the total spectral energy

$$E=\int_0^{\infty}F(k)\mathrm{d}k\approx\frac{\alpha}{2}\int_{k_p}^{\infty}k^{-3}\mathrm{d}k \tag{6}$$

Introducing non-dimensional variables, Eq. (6) can be integrated to yield

$$\epsilon=\frac{\alpha}{4}\kappa^{-2} \tag{7}$$

where $\kappa=U_{10}^2 k_p/g$ is the non-dimensional peak wavenumber, $\epsilon=Eg^2/U_{10}^4$ is the non-dimensional energy and k_p is the wave number of the spectral peak. Bouws et al. (1985) demonstrated that Eq. (7) was a good approximation to the observed data, supporting the applicability of the TMA form, Eq. (4).

Bouws et al. (1987) examined the evolution of the spectral parameters, α, γ and σ. They found that α was an increasing function of κ although there was significant scatter in their data. They approximated this relationship by a power law. In a similar fashion to JONSWAP (Hasselmann et al., 1973) the peak shape parameters γ and σ exhibited significant scatter with no clear trends.

A further application of the general theory of Kitaigorodskii (1962) was applied by Miller and Vincent (1990). Rather than adopting the k^{-3} scaling of Eq. (3), they proposed a form proportional to $k^{-2.5}$ which transforms to a deep water frequency spectrum proportional to f^{-4}. This form was compared with data from the Corps of Engineers Field Research Facility on the east coast of the United States. They found that this form, when transformed to frequency space (termed the FRF spectrum), modelled the data equally well as the TMA form. They also found that the spectral parameters of α and σ were relatively constant for this spectral formulation. In addition, a correlation existed between γ and the wave steepness ($\Lambda = \sqrt{E}/L_p$, where E is the total energy and L_p is the wave length of components at the spectral peak). It should be noted, however, that Λ has only a relatively small dynamic range for typical condition and hence such a correlation should be treated with some caution.

An alternative approach has been proposed by Thornton (1977) in which the wave celerity is the governing parameter at high frequencies. Using similarity arguments a general spectral form is derived which is of the form f^{-5} in deep water and f^{-3} in shallow water. These asymptotic limits are consistent with Kitaigorodskii (1962).

3. Data selection and processing

A full description of the present experimental configuration and instrumentation used is contained in Part 1. In summary, however, the experiment consisted of the measurement of water surface elevation and wind speed and direction at a series of eight stations with fetches ranging from 1.3 km to 16 km in a lake of relatively uniform water depth of approximately 2 m. In the present paper only data for which the wind direction was within 20° of the array alignment has been considered. In this manner slanting fetch conditions have been excluded. In addition, only cases for which the wind speed and direction are relatively constant have been retained (see Part 1 for details).

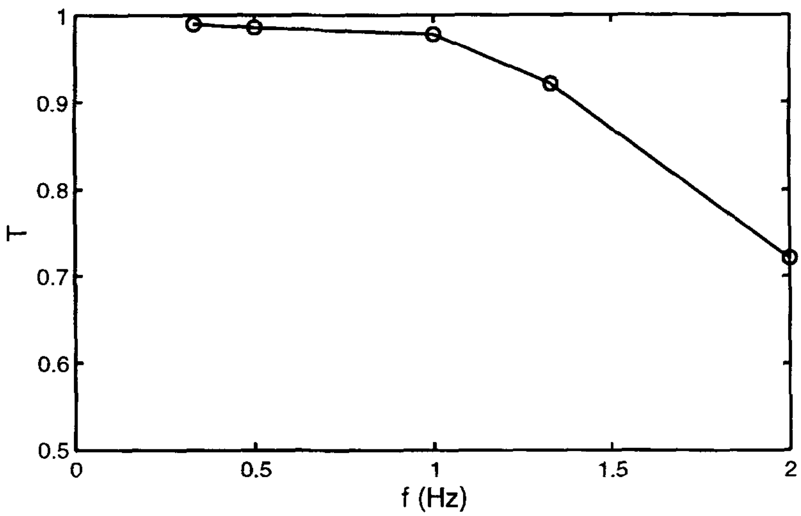

Fig. 1. Zwarts pole transfer function obtained by oscillating the sensing element vertically in still water.

The water surface elevation was measured at each of the stations using surface piercing Zwarts poles (Zwarts, 1974). Thirty minute time series were recorded for each of the poles, leading to time series of 14,400 points. The time series were sub-divided into 256 point sections, passed through a Hanning window, and energy spectra determined using ensemble averages of the sub-divided time series. The resulting spectra have 112 degrees of freedom, a Nyquist frequency of 4 Hz and a frequency resolution of 0.031 Hz.

The construction of the Zwarts poles consists of two concentric tubes with holes in the outer tube allowing water to enter the sensing annulus. The restriction to flow represented by the holes and the physical size of the pole (outer diameter 50 mm) obviously degrades instrument performance at high frequencies. During the instrument design phase a series of dynamic calibrations were conducted to optimize the number and configuration of these holes. Poles were oscillated vertically in still water using a pulley and eccentric cam system whilst the position of the pole and the output from the pole were coincidently logged. The results of these calibrations for the final hole configuration are shown in the transfer function of Fig. 1. Fig. 1 shows that the transfer function is relatively flat for frequencies less than approximately 1.2 Hz but rapidly decays above this point.

As there was some doubt as to whether oscillating the poles in still water accurately represented the flow éxperienced by the poles, in situ comparisons were performed against twin wire resistance waves gauges. The wave gauges were sampled at the higher rate of 20 Hz to also investigate whether aliasing effects were significant at the lower 8 Hz sampling rate used for the Zwarts poles. A total of 18 intercomparisons were

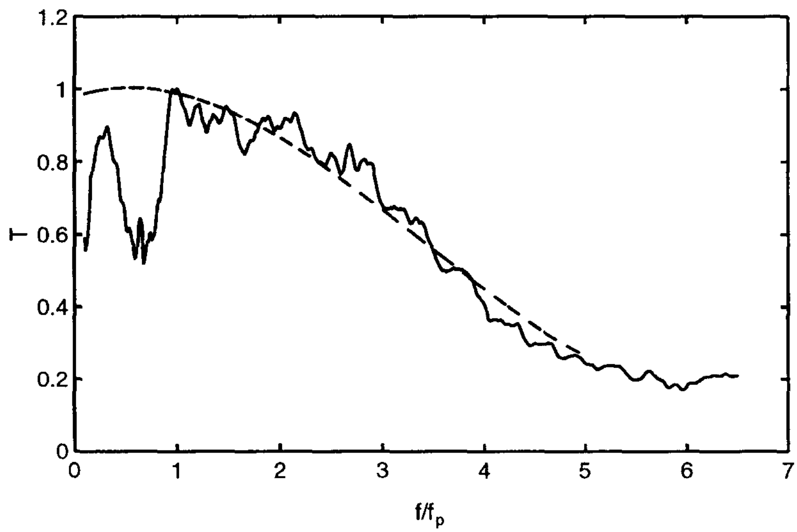

Fig. 2. Zwarts pole transfer function obtained from insitu comparisons with a twin wire resistance gauge. Results are presented in terms of f/f_p. The dashed line represents the polynomial approximation used during the data reduction procedure.

conducted at wind speeds ranging from 5 m/s to 14 m/s. Intercomparison of the resulting transfer functions showed that the frequency response was poorer than indicated by the laboratory dynamic calibrations. In addition, the transfer function was not simply a function of frequency. Over the wide range of conditions tested, the transfer

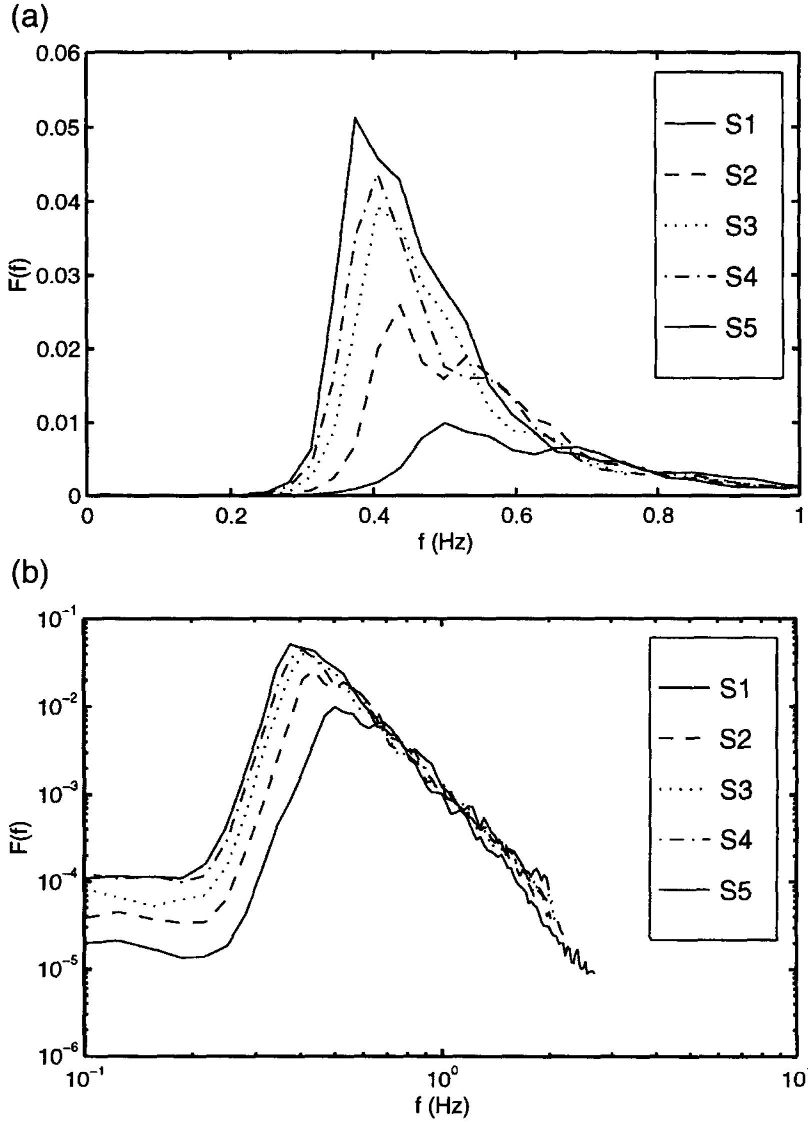

Fig. 3. An example of the development of the wave spectra with increasing fetch. The stations are labelled S1 to S5 (increasing fetch, see Part 1). Spectral evolution at fetches larger than S5 is very small and hence these spectra have been omitted for clarity. The case shown is for a northerly wind measured at S6 of $U_{10} = 10.8$ m/s. Panel (a) shows a linear scale whilst panel (b) is a logarithmic scale.

functions appeared to depend on the position of the spectral peak, and could be expressed in terms of f/f_p. We attribute this to the fact that it is the vertical velocity of the water surface that limits the instrument performance. The high frequency waves are superimposed on the longer waves near the spectral peak. Thus the local water surface slope (and the vertical velocity) is influenced by all spectral components, not simply a single spectral component as assumed in the laboratory tests. The transfer function, averaged over all 18 tests and scaled in terms of f/f_p is presented in Fig. 2. The transfer function was represented by a polynomial approximation as shown in Fig. 2. At frequencies above $5f_p$ output from the Zwarts poles appeared flat, indicating an upper frequency limit to instrument response. To account for the frequency response of the poles, all recorded spectra were corrected using the polynomial approximation to the transfer function and truncated at $5f_p$.

Fig. 3 shows a typical example of the measured spectral evolution. The case shown in Fig. 3 was for a northerly wind of 10.8 m/s as measured at Station 6. As shown in Part 1, the wind speed increases down the fetch as an internal boundary layer develops over the aerodynamically smooth lake surface. The spectra of Fig. 3 clearly show the self-similarity of the spectra previously observed in deep water studies. The increase in total energy of the spectra and the migration of the spectral peak to lower frequencies are clearly evident in this figure. As observed in deep water, the high frequency portion of the spectrum appears reasonably well approximated by a relationship of the form $F(f) \propto f^n$. Close examination of the spectra, however, suggests that n may change with increasing fetch (see Section 4).

4. High frequency region

For frequencies above the spectral peak frequency, f_p, the JONSWAP form (Eq. (1)) yields the result $F(f) \propto f^{-5}$ and the Donelan et al. (1985) form (Eq. (2)), $F(f) \propto f^{-4}$. The TMA form (Eq. (4)), yields a high frequency form which has a variable exponent of f, increasing in magnitude with increasing f. To investigate the most appropriate high frequency spectral form, an equation of the form $F(f) = \beta f^n$ was fitted using the method of least squares for the spectral region $f > 2f_p$. The fit was applied to all (approximately 1,000) spectra in the north/south data set. Rather than the exponent being a universal constant, as predicted by either Eq. (1) or Eq. (2), it appeared to vary as a function of non-dimensional fetch, χ and non-dimensional depth, δ. The values of the resulting exponent, n are shown in Fig. 4 as a function of χ. The data have been partitioned into two ranges: $\delta = 0.1$–0.2 and $\delta = 0.5$–0.6. The results show that at short non-dimensional fetch, n is approximately equal to -5. As the fetch increases the value of the exponents changes and at the longer non-dimensional fetches n approximates -3. At short non-dimensional fetch, the waves are in deep water, the effects of finite depth increasing as the non-dimensional fetch increases and the waves develop. Hence, the gradual decrease in the magnitude of the exponent appears to be associated with the effects of finite depth. This is further supported by the fact that for the same value of χ, the deeper data (larger δ) yield values of n of larger magnitude than the shallower data

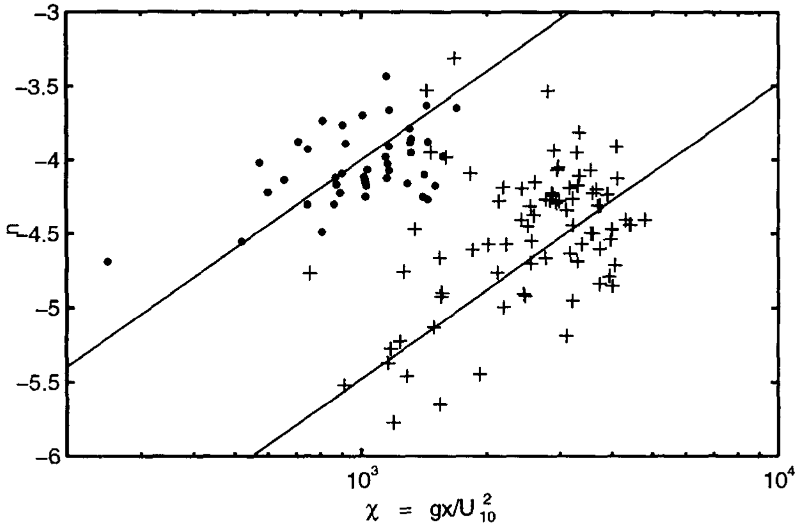

Fig. 4. Values of the high frequency exponent, n (Eq. (8)) as a function of non-dimensional fetch, χ. Data for two ranges of non-dimensional depth, δ are shown, $0.1 < \delta < 0.2$ (dots) and $0.5 < \delta < 0.6$ (crosses). The solid lines are visual trend lines showing the decrease in the magnitude of n as finite depth effects become more significant.

(smaller δ). As δ increases, finite depth effects will only become significant at larger values of χ.

5. Finite depth spectral form

As outlined in Section 4, the data suggest that the high frequency exponent varies with water depth. Such a result is consistent with the proposed TMA spectral form (Bouws et al., 1987). Other spectral forms based on the general JONSWAP shape can also be proposed with a variable high frequency exponent. One generalized form is

$$F(f) = \alpha g^2 (2\pi)^{-4} f_p^{-(5+n)} f^n \exp\left[\frac{n}{4}\left(\frac{f}{f_p}\right)^{-4}\right] \cdot \gamma^{\exp\left[\frac{-(f-f_p)^2}{2\sigma^2 f_p^2}\right]} \tag{8}$$

For $n = -5$ this result reduces to JONSWAP, (1), whereas for $n = -4$ it yields the form of Donelan et al. (1985), Eq. (2). Both Eq. (8) and the TMA form (Eq. (4)) will be investigated as possible representations of the measured spectra.

A variety of techniques have been proposed for fitting the multi-parameter, non-linear forms represented by Eq. (4) or Eq. (8) (Günther, 1981; Battjes et al., 1987; Donelan et al., 1985). All of these methods have involved the use of piecewise techniques where each of the spectral parameters are determined separately. An alternative approach is to use a multi-parameter, non-linear least squares curve fitting technique (e.g. the Levenberg-Marquardt method, Press et al., 1986) and determine all the parameters simultaneously. In an ideal situation, where the spectrum conforms perfectly to the proposed spectral form, both approaches will yield identical results. In reality, measured spectra are prone to sampling variability and the fitting technique must recover the spectral parameters in the presence of this sampling "noise" and with spectral data defined on a relatively coarse frequency grid.

In order to investigate the most appropriate technique, a Monte-Carlo simulation of the proposed techniques was performed. A mean spectrum of the TMA form (Eq. (4)) was defined with spectral parameters typical of those for the present situation. The spectrum was defined on the same discrete frequency grid resulting from the Fourier analysis used to determine the measured spectra. Each of the ordinates of this analytical spectrum was allowed to vary about the mean value whilst following a chi-squared probability distribution with 112 degrees of freedom (typical of recorded spectra, see Section 3). In addition, the discrete frequency grid was varied by an amount Δf assuming a uniform distribution (see Young, 1996). A total of 10,000 realizations of the spectrum were generated following this approach and the ability of the curve fitting techniques to recover the know spectral parameters investigated.

Fig. 5 shows the results for each of the techniques in the form of distribution histograms. It is clear that the multi-parameter fit yields results which are unbiased and symmetrically distributed about the mean values. In contrast, the piecewise technique (Donelan et al., 1985) yields results which are marginally biased. In the mean it yields values of α which are approximately 3% to small and γ which are 12% to high. Consequently, the multi-parameter technique has been adopted for the remainder of this analysis.

Both spectral forms, Eq. (4) and Eq. (8), were fitted to all spectra in the north/south data set. An indication of how well these spectral forms approximate the observed spectra can be obtained by determining the following rms error statistics

$$E_1 = \left[\frac{1}{N} \sum_{i=1}^{N} e_i^2 \right]^{1/2} \tag{9}$$

$$E_2 = \left[\frac{1}{(N-P+1)} \sum_{i=P}^{N} e_i^2 \right]^{1/2} \tag{10}$$

where N specifies the number of spectral bands in the analyzed spectra and P is the index number of the frequency band of the spectral peak. The quantity e_i is defined as

$$e_i = \frac{F_i(\text{fit}) - F_i(\text{data})}{F_i(\text{data})} \tag{11}$$

where F_i(fit) indicates the ith spectral ordinate of the analytical spectral form fitted to the data and F_i(data), the corresponding ordinate of the measured spectrum.

Eq. (9) gives an indication of how well the analytical form approximates the data over the full spectrum, whereas Eq. (10) indicates the appropriateness of the fit in the high frequency region. When averaged over the full 1,000 spectra in the data set, Eq. (4)

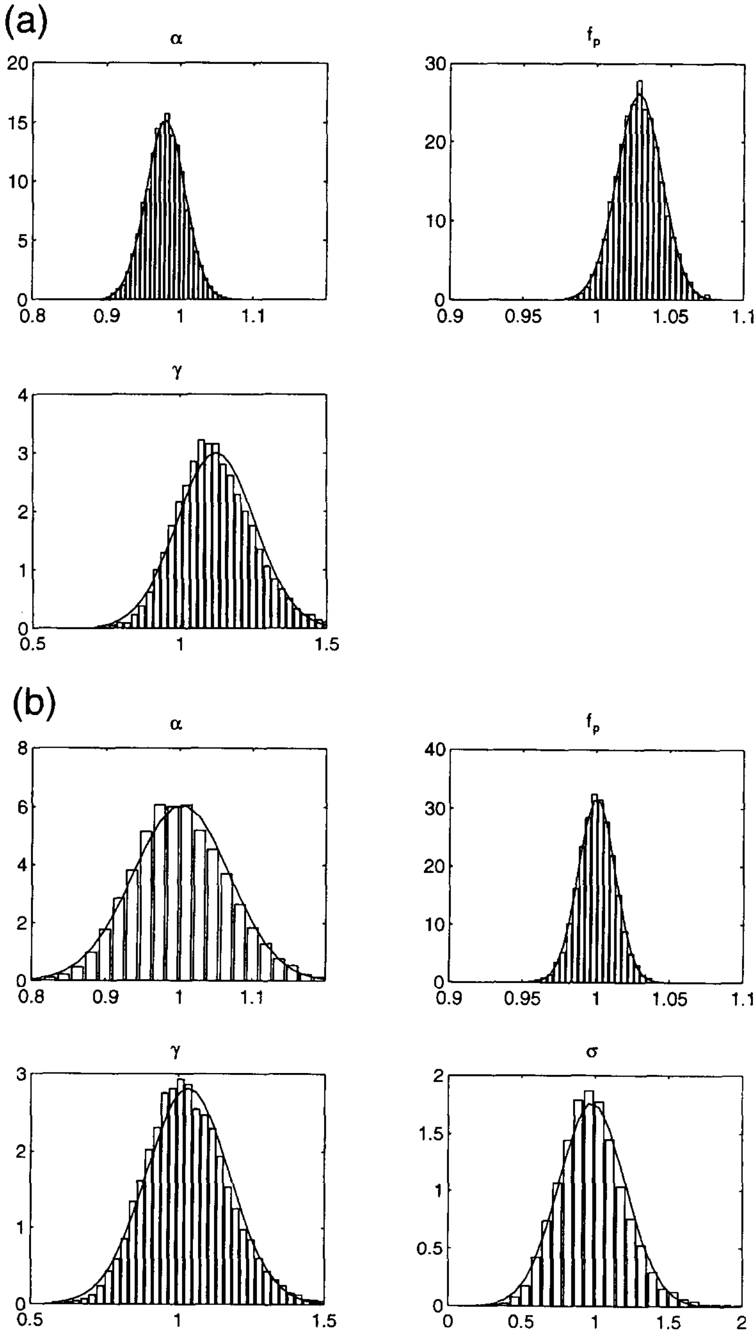
(a)
α
f_p
γ
(b)
α
f_p
γ
σ

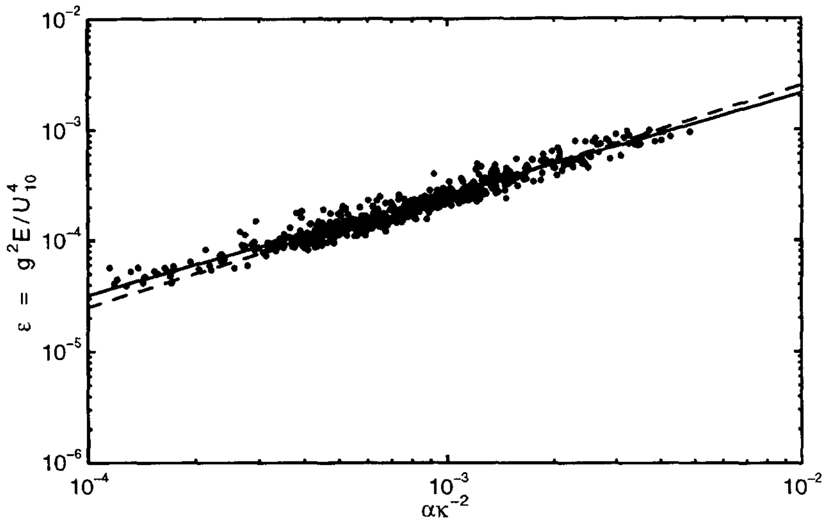

Fig. 6. Values of the non-dimensional energy, ϵ as a function of the quantity, $\alpha\kappa^{-2}$. The solid line is a least squares fit to the data (Eq. (12)) whereas the TMA form (Eq. (7)), which ignores the contribution of spectral enhancement, is shown by the dashed line.

(i.e. TMA) yielded values of $E_1 = 0.24$ and $E_2 = 0.19$ compared to Eq. (8) with $E_1 = 0.37$ and $E_2 = 0.36$. Eq. (8) has one more free parameter (n) than Eq. (4). Despite this, the error statistics indicate it is a poorer approximation to the data than the more constrained TMA form (Eq. (4)). This is a clear indication that the high frequency spectral region of these finite depth spectra is not well approximated by a form f^n, where n is a constant. Due to the Φ term in Eq. (4), the resulting high frequency exponent is frequency dependent, increasing in magnitude with increasing frequency. Hence, it can be concluded that the TMA spectral form (Eq. (4)) is a better approximation than a form with a constant exponent high frequency region (i.e. JONSWAP, Hasselmann et al., 1973; Donelan et al., 1985 or even a general form such as Eq. (8)).

Further evidence that the observed spectra are well represented by the TMA form is provided by Fig. 6 which shows the non-dimensional energy, ϵ as a function of the quantity $\alpha\kappa^{-2}$, where α and κ were determined from the multi-parameter fit of Eq. (4) to the observed spectra. Based on Kitaigorodskii (1962) scaling, and disregarding the contribution of peak enhancement to the total spectral energy, Eq. (7) indicates

---

Fig. 5. (a) The distribution of values of the spectral parameters for Eq. (4) obtained from a Monte-Carlo simulation with a piecewise fitting technique (i.e. parameters are fitted successively). Panel (i) shows α, (ii) f_p, (iii) γ. The parameter σ is not shown as it was considered constant in this fitting process. b. The distribution of values of the spectral parameters for Eq. (4) obtained from a Monte-Carlo simulation with a simultaneous multi-parameter fitting technique. Panel (i) shows α, (ii) f_p, (iii) γ and (iv) σ.

$\epsilon \propto \alpha\kappa^{-2}$. The data are remarkably well approximated by this relationship (see Fig. 6), a regression analysis yielding

$$\epsilon = 0.14(\alpha\kappa^{-2})^{0.91} \tag{12}$$

The above results provide strong support for a wavenumber spectral form $F(k) \propto k^{-3}$ and its transformation to a frequency spectrum with the TMA form as the appropriate spectral function in water of finite depth.

6. Evolution of spectral parameters

Based on the wavenumber scaling arguments implicit in the TMA spectral form, Bouws et al. (1985, 1987) speculated that the spectral parameters should be functions of the non-dimensional wavenumber, κ. To investigate this dependence with the present data set, the spectral parameters of α, γ and σ are presented as functions of κ in Figs. 7–9, respectively. As with previous studies of spectral evolution, there is significant scatter in the data. This feature is investigated with a detailed error analysis in Section 8.

Within the data scatter, a relationship between α and κ is clear, with α an increasing function of κ (see Fig. 7). A least squares fit to the data yields the power law relationship

$$\alpha = 0.0091\kappa^{0.24} \tag{13}$$

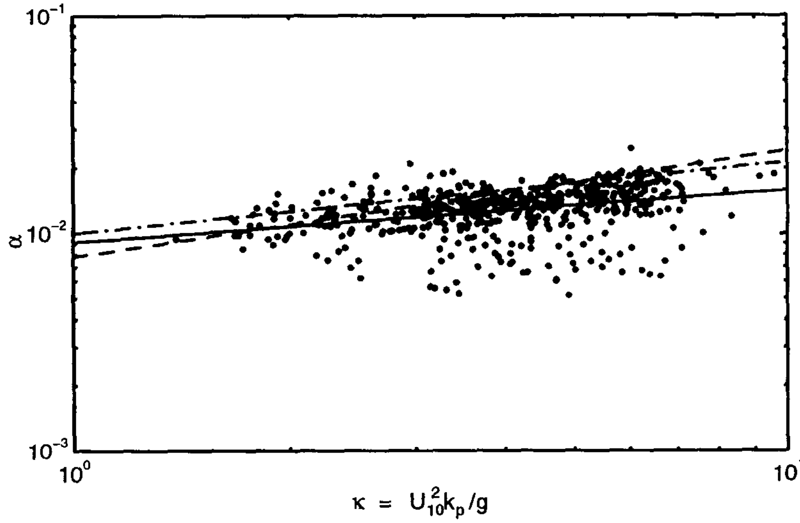

Fig. 7. Values of the parameter α as a function of non-dimensional wavenumber, κ. The solid line is a least squares fit to the data (Eq. (13)). The TMA result is shown by the dashed line and the JONSWAP form, transformed from frequency to wavenumber space, by the dash–dot line.

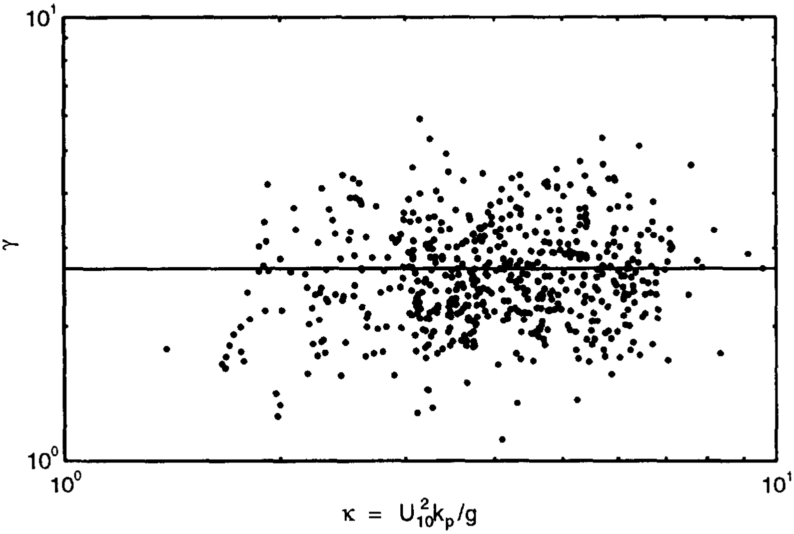

Fig. 8. Values of the peak enhancement parameter, γ as a function of non-dimensional wavenumber, κ. The horizontal line represents the data mean.

Eq. (13) is shown on Fig. 7, together with the TMA result, $\alpha_{TMA} = 0.0078\kappa^{0.49}$. Both Eq. (13) and the TMA form are consistent with the data. In deep water the general TMA form reverts to that of JONSWAP. The deep water JONSWAP result scales α in terms of the non-dimensional frequency, ν, $\alpha_{JONSWAP} = 0.033\nu^{0.67}$. Assuming a deep water

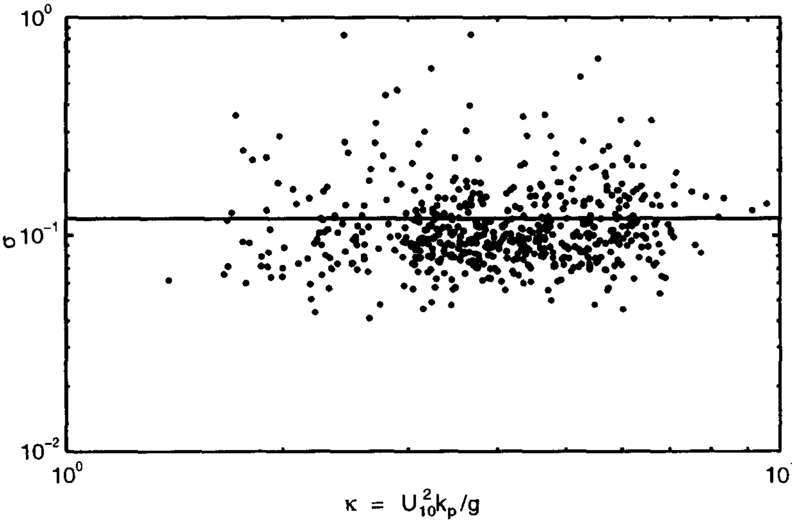

Fig. 9. Values of the spectral parameter, σ as a function of non-dimensional wavenumber, κ. The horizontal line represents the data mean.

linear dispersion relationship, this result can be converted to wavenumber space, $\alpha_{JONSWAP} = 0.01\kappa^{0.33}$. This JONSWAP result is also shown in Fig. 7 and is broadly consistent with the finite depth formulations.

All results are comparable and confirm that the trend towards decreasing values of α with increasing maturity of the waves, already observed in deep water, also holds in finite depth situations.

In contrast to the observable trend in α with κ, no similar result is apparent for either γ or σ. This result is consistent with both TMA (Bouws et al., 1985, 1987) and JONSWAP (Hasselmann et al., 1973). As will be shown in Section 8 there is, however, significant sampling variability associated with these parameters. The mean values of the data set yield $\gamma_{mean} = 2.70$ and $\sigma_{mean} = 0.12$.

7. Consistency of results

The results given in Section 6, together with the TMA form (Eq. (4)), fully define the spectrum. Integration of this spectral form yields the total energy, E. This total energy can also be determined independently from the results given in Part 1. If E is determined using these two approaches, for the range of parameters observed during the experiment, in the mean, the results agree. In some regions of the parameter space, however, a discrepancy in the values of E determined by the two approaches of up to 30% exists. This inconsistency between the results is attributed to the rather unsatisfactory dependence of γ on κ. Adoption of simply the mean value for γ potentially masks

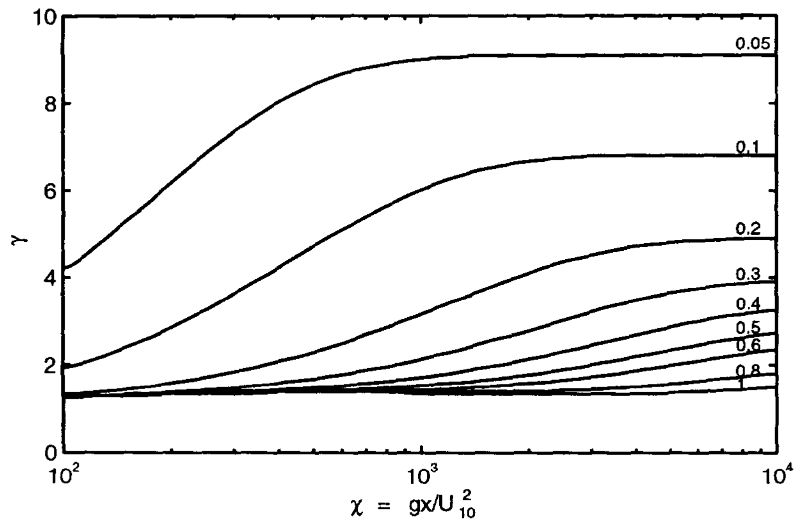

Fig. 10. Values of the peak enhancement parameter γ as a function of non-dimensional fetch, χ for various values of non-dimensional depth, δ. Values were determined using the growth relationships derived in Part 1, together with α obtained from Eq. (13) and a constant mean value of $\sigma = 0.12$ (i.e. data mean). The values of δ for each line are shown at the right extreme of the figure.

a dependence on other parameters. A similar argument also holds for σ. Variations in σ, however, have an insignificant influence on the total energy, E and have been neglected, simply excepting the mean value as representative.

To investigate whether there is a systematic dependence of γ on other parameters, the problem has been inverted. For given values of non-dimensional fetch, χ and non-dimensional depth, δ, the relationships in Part 1 yield corresponding non-dimensional energy, ϵ and non-dimensional peak frequency, ν. Given δ and ν, the non-dimensional peak wavenumber, κ can be determined with the aid of the linear dispersion relationship. With κ known, α can be evaluated from Eq. (13) and the mean value for σ can be assumed. An iterative approach was then adopted to determine the value of γ required to produce a spectrum which upon, integration, yields a value of ϵ equal to that originally obtained from the Part 1 relationship.

The resulting values of γ are presented as functions of χ and δ in Fig. 10. The results in Fig. 10 show a clear trend in γ as a function of χ and δ. For a given value of δ, as χ increases and the effects of finite depth increase, the value of γ increases significantly. It can be concluded that the spectra of severely depth limited spectra are very peaked. Visually, such peaked spectra should appear quite ordered and monochromatic, a large percentage of the spectral energy being concentrated near a single frequency. Indeed, our visual observations confirm this result. During high wind conditions (and hence depth limited), the waves were distinctly long crested with a clearly discernible dominant period. This differs markedly from conditions observed during less severely forced situations, where the resulting wave field was extremely confused. This made operations on the lake in small boats extremely difficult.

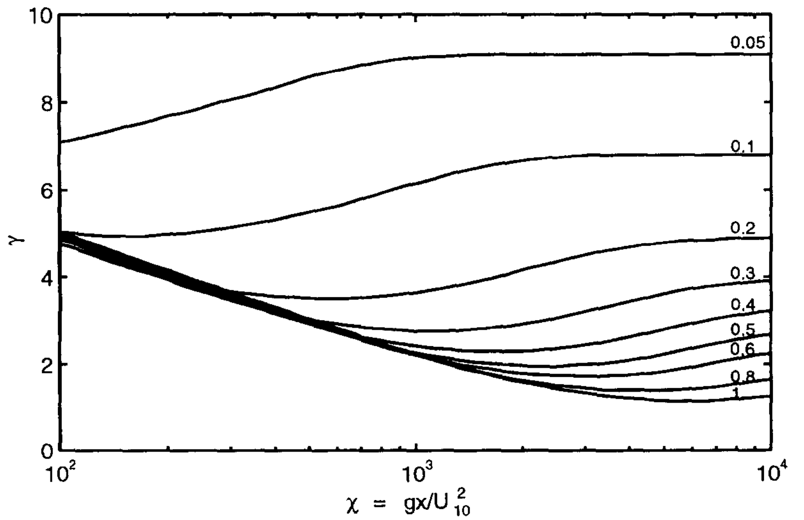

Fig. 11. Values of the peak enhancement parameter γ as a function of non-dimensional fetch, χ for various values of non-dimensional depth, δ. The values were obtained using the same process as in Fig. 10, except that the JONSWAP results were used as a deep water asymptote for the non-dimensional frequency, γ, rather than the Kahma and Calkoen (1992) form adopted in Part 1. The values of δ for each line are shown at the right extreme of the figure.

The results in Fig. 10, indicate that γ decreases as δ increases. At the deep water limit, γ approaches a value only slightly larger than unity and is relatively constant with fetch. This result appears inconsistent with previous deep water results. Although they could find no trend in their data, Hasselmann et al. (1973) found a mean value of 3.3 for γ. Although Donelan et al. (1985) investigated a different spectral form (Eq. (2)), they found that γ decreased with fetch in deep water. The present results occur due to the assumed deep water asymptotic form for the growth curves adopted in Part 1. Here the growth curve for non-dimensional energy asymptotes to JONSWAP for deep water, whereas that for non-dimensional frequency asymptotes to that proposed by Kahma and Calkoen (1992). If a JONSWAP asymptotic form had been adopted for non-dimensional frequency, a rather different result would have been obtained as shown in Fig. 11. The depth limited variation in γ is still identical to that in Fig. 10, but the deep water behaviour is now quite different. The deep water asymptote now shows γ decreasing with increasing fetch. Although this result is more consistent with previous deep water findings, the relationship of Kahma and Calkoen (1992) was in far better agreement with the observed data than that of JONSWAP. For this reason, we leave the transition of γ from deep to depth limited conditions as an open question. The depth limited behaviour of γ, however, appears well defined by the data.

Fig. 12 shows γ for depth limited conditions as a function of non-dimensional water depth, δ. A clear trend develops with γ decreasing as δ increases. A least squares fit to these data yields

$$\gamma_{\mathrm{dl}} = -5.8\log_{10}\delta + 1.1 \quad \text{for } 0.05 < \delta < 1 \tag{14}$$

where the subscript "dl" is included to signify that this is the depth limited value.

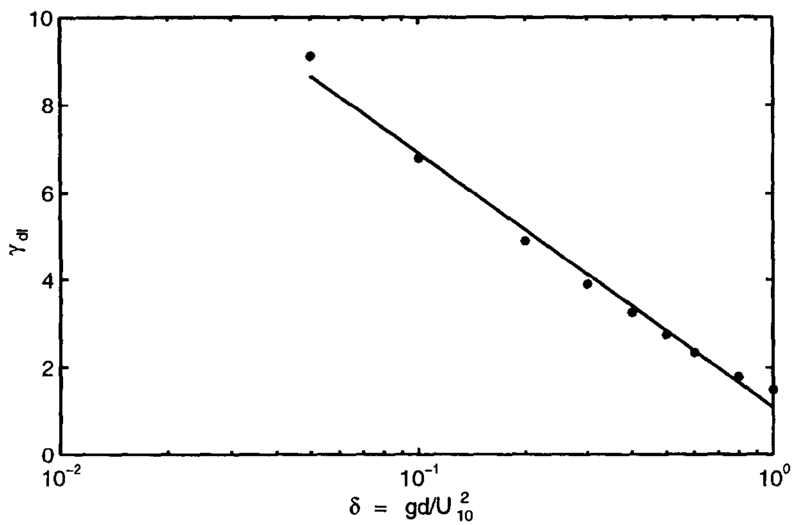

Fig. 12. Depth limited values of the parameter, γ as a function of non-dimensional depth, δ (i.e. the values shown in Fig. 10 and Fig. 11 at large χ). The derived values are shown by the dots, with the least squares fit to the data (Eq. (14)) represented by the solid curve.

In deep water, one consequence of γ decreasing with fetch is the observed "overshoot" at frequencies immediately above the spectral peak. Since the present finite depth data exhibit the opposite trend for γ, no overshoot would be expected. This is confirmed by an examination of the spectra in Fig. 3.

8. Error analysis

The results shown in Figs. 6–9 exhibit significant scatter in the derived spectral parameters. It is prudent to investigate whether this scatter is consistent with the natural sampling variability which could be expected or whether it is an indicator of an inappropriate spectral form. In order to investigate the influence of sampling variability, a Monte-Carlo simulation, as in Section 5, was performed. A TMA spectral form (Eq. (2)) was assumed with parameters typical of those observed in the present data ($\alpha = 0.01$, $f_p = 0.4$ Hz, $\sigma = 0.1$, $\gamma = 2.5$ and $d = 1.8$ m). The spectrum was defined on a discrete spectral grid with a resolution $\Delta f = 0.031$ Hz, as used in the data processing (see Section 3). The ordinates of the spectrum were considered to be statistical variables, with a mean given by the assumed TMA form, but following a chi-squared probability distribution. In addition, the position of the discrete frequency grid was allowed to vary by an amount equal to Δf, following a uniform distribution. In this manner, the position of the spectral peak relative to the discrete values of the frequency axis is considered in the analysis. A total of 10,000 realizations of the spectrum were determined, the multi-parameter least squares technique being used to determine the spectral parameters for each realization.

For all parameters, values followed approximately normal distributions with distribution means almost identical to the mean values of the initial spectral shape (see Fig. 5). This indicates that the spectral fitting technique is unbiased. For each of the parameters, the 10,000 values were ordered and the 2.5 and 97.5 percentile values determined. The resulting span of values defines the 95% confidence limits and are shown in Table 1.

The difficulty of accurately determining the spectral peak shape parameters of γ and σ is clear in Table 1, with very large variability in these parameters. It is clear from this table that a significant percentage of the scatter observed in the derived spectral parameters is as a result of the statistical variability of the spectra. The remaining scatter is presumably due to effects such as wind speed and water depth variability as well as irregularities of the down wind shore line. Other influences such as atmospheric stability may also influence the results.

Table 1
Sampling variability of the TMA spectral parameters expressed in terms of the span of values making up the 95% confidence limits. Value were determined from a Monte Carlo simulation

Parameter	Span of 95% confidence limit
α	$\pm 13\%$
f_p	$\pm 2.5\%$
γ	$\pm 28\%$
σ	± 44

9. Conclusions

The experimental results presented in this paper represent the first detailed investigation of the development of finite depth wave spectra with fetch. The results clearly demonstrate that the high frequency tail of the spectra cannot be represented by a simple exponential form as in deep water. The appropriate exponent varies as a function of water depth. In deep water this exponent is approximately -5, whereas in extremely depth limited situations it approaches, -3 (Kitaigorodskii, 1962; Thornton, 1977). In addition, even a spectral form with a variable high frequency exponent is not a good approximation to the observed spectra. The high frequency spectral decay gradually "steepens" as a function of frequency. This occurs as the high frequency (short period) spectral components are essentially in deep water whereas the lower frequency (longer period) components near the spectral peak are more influenced by the water depth. These results are consistent with the previously proposed TMA (Bouws et al., 1985) spectral form, which is found to be a good approximation to the data.

As proposed by Bouws et al. (1985, 1987) the spectral parameter, α is found to be a function of the non-dimensional wavenumber, κ (Eq. (13)). In contrast, the spectral shape parameters, γ and σ are uncorrelated with κ. The value of σ has little practical significance, as it has only a small influence on the total spectral energy and the mean value of $\sigma_{mean} = 0.12$ seems appropriate for engineering applications. The peak enhancement factor, γ, however has a moderate influence on the total spectral energy. Unfortunately, the data set is insufficient to fully resolve the transition of γ from deep to depth limited situations (even the previous deep water experiments have produced no consistent understanding of the variation in γ). In depth limited situations, however, γ appears to be a function of the non-dimensional water depth, δ (Eq. (14)). The value of γ increases as δ decreases. Hence, severely depth limited spectra could be expected to be very peaked. This result is consistent with our visual observations.

It is interesting that the present data set, which was obtained from a lake with a cohesive mud bottom, is consistent with the mobile bed ocean data of the composite TMA experiments (Bouws et al., 1985). As in Part 1, we speculate that this insensitivity to bed material indicates that bottom friction dissipation is not significant in finite depth fetch limited growth.

Acknowledgements

Numerous members of the technical staff of the School of Civil Engineering, University College, UNSW have made enormous contributions to the success of this large field experiment. Mary Dalton and Peter McMahon of our electronics section have designed and constructed all electronics used in the project, the reliability of the instrumentation speaks volumes for their skills. The support towers, central platform and numerous other components were constructed by John MacLeod, Doug Collier and Bernie Miller. In addition, numerous other members of staff have assisted in the deployment and maintenance of instruments. They include: Graham Johnston, Jon Delaney, Terry Lutze, David Sharp and Jim Baxter. The project could not have been successful without the significant contributions from this large and very skilled group of people. The project was funded by the Australian Research Council, without which it would have been impossible. This contribution is gratefully acknowledged.

References

Banner, M.L., 1990. Equilibrium spectra of wind waves. J. Phys. Oceanogr., 20: 966–984.

Banner, M.L. and Young, I.R., 1994. Modelling spectral dissipation in the evolution of wind waves — Part 1. Assessment of existing model performance. J. Phys. Oceanogr., 24: 1550–1671.

Battjes, J.A., Zitman, T.J. and Holthuijsen, L.H., 1987. A reanalysis of the spectra observed in JONSWAP. J. Phys. Oceanogr., 17: 1288–1295.

Bouws, E., 1986. Provisional results of a wind wave experiment in a shallow lake (Lake Marken, The Netherlands). KNMI Afdeling Oceanografisch Onderzoek, OO-86-21, De Bilt, 15 pp.

Bouws, E., Günther, H., Rosenthal, W. and Vincent, C.L., 1985. Similarity of the wind wave spectrum in finite depth water, 1. Spectral form. J. Geophys. Res., 90: 975–986.

Bouws, E., Günther, H., Rosenthal, W. and Vincent, C.L., 1987. Similarity of the wind wave spectrum in finite depth water, 2. Statistical relationships between shape and growth stage parameters. Dtsch. Hydrogr. Z., 40: 1–24.

Bretschneider, C.L., 1958. Revised wave forecasting relationships. In: Proc. 6th Conference on Coastal Engineering, Gainesville/Palm Beach/Miami Beach, FL. ASCE, New York, pp. 30–67.

Donelan, M.A., Hamilton, J. and Hui, W.H., 1985. Directional spectra of wind-generated waves. Philos. Trans. R. Soc. London, A315: 509–562.

Forristall, G.Z., 1981. Measurements of a saturation range in ocean wave spectra. J. Geophys. Res., 86: 8075–8084.

Günther, H., 1981. A parametric surface wave model and the statistics of the prediction parameters. Hamburger Geophysikalishe Einzelschriften, 90 pp.

Hasselmann, K. et al., 1973. Measurements of wind-wave growth and swell decay during the Joint North Sea Wave Project (JONSWAP). Dtsch. Hydrogr. Z. Suppl. A, 8(12), 95 pp.

Kahma, K.K., 1981. A study of the growth of the wave spectrum with fetch. J. Phys. Oceanogr., 11: 1503–1515.

Kahma, K.K. and Calkoen, C.J., 1992. Reconciling discrepancies in the observed growth of wind-generated waves. J. Phys. Oceanogr., 22: 1389–1405.

Kitaigorodskii, S.A., 1962. Applications of the theory of similarity to the analysis of wind-generated wave motion as a stochastic process. Izv. Akad. Nauk SSSR, Geophys. Ser., 1: 105–117.

Kitaigorodskii, S.A., 1983. On the theory of the equilibrium range in the spectrum of wind-generated gravity waves. J. Phys. Oceanogr., 13: 816–827.

Kitaigorodskii, S.A., Krasitskii, V.P. and Zaslavskii, M.M. , 1975. On Phillips' theory of equilibrium range in the spectra of wind-generated gravity waves. J. Phys. Oceanogr., 5: 410–420.

Miller, H.C. and Vincent, C.L., 1990. FRF spectrum: TMA with Kitaigorodskii's f^{-4} scaling. ASCE J. Waterw. Port Coastal Ocean Div., 116: 57–78.

Mitsuyasu, H., Tasai, F., Suhara, T., Mizuno, S., Onkusu, M., Honda, T. and Rukiiski, K., 1975. Observations of the directional spectrum of ocean waves using a cloverleaf buoy. J. Phys. Oceanogr., 5: 751–761.

Phillips, O.M., 1958. The equilibrium range in the spectrum of wind-generated waves. J. Fluid Mech., 4: 426–434.

Pierson, W.J. and Moskowitz, L., 1964. A proposed spectral form for fully developed wind seas based on the similarity theory of S.A. Kitaigorodskii. J. Geophys. Res., 69(24): 5181–5190.

Press, W.H., Flannery, B.P., Teukolsky, S.A. and Vetterling, W.T., 1986. Numerical Recipies. Cambridge University Press, 818 pp.

Resio, D.T., 1987. Shallow-water waves I: Theory. ASCE J. Waterw. Port Coastal Ocean Eng., 113: 264–281.

Thornton, E.B., 1977. Rederivation of the saturation range in the frequency spectrum of wind-generated gravity waves. J. Phys. Oceanogr., 7: 137–140.

Toba, Y., 1973. Local balance in the air–sea boundary processes. Part III: On the spectrum of wind waves. J. Oceanogr. Soc. Jpn., 29: 209–220.

U.S. Army Corps of Engineers, 1955. Waves and wind tides in shallow lakes and reservoirs. Summary Report, Project CW-167, Jacksonville District, FL.

Young, I.R., 1996. The determination of confidence limits associated with estimates of the spectral peak frequency. Ocean Eng., in press.

Young, I.R. and Van Vledder, G. Ph., 1993. A review of the central role of nonlinear interactions in wind-wave evolution. Philos. Trans. R. Soc., 342: 505–524.

Young, I.R. and Verhagen, L.A., 1996. The growth of fetch limited waves in water of finite depth. Part 1. Total energy and peak frequency. Coastal Eng., 29 (1996) 47–78 (this issue).

Zwarts, C.M.G., 1974. Transmission line wave height transducer. In: Int. Symp. on Wave Measurement and Analysis, pp. 605–620.